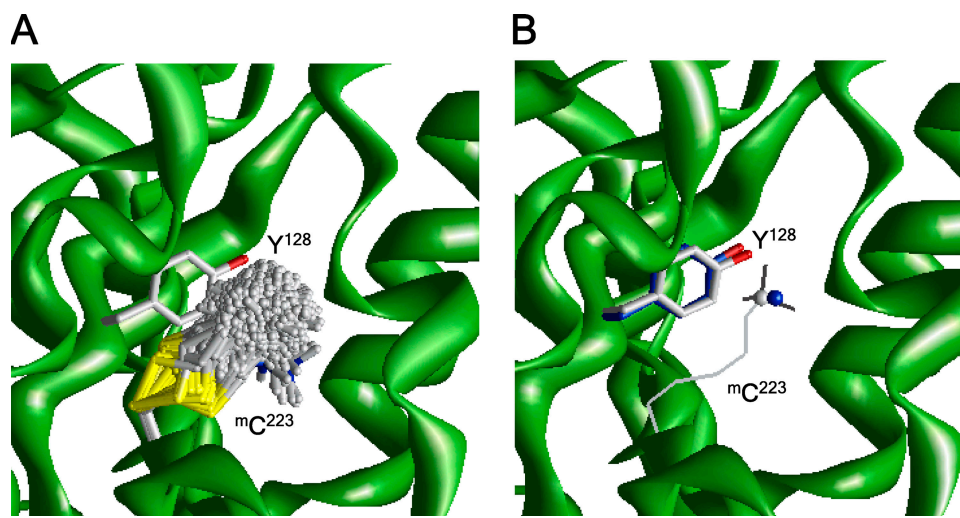


Bruhova and Zhorov, <http://www.jgp.org/cgi/content/full/jgp.200910288/DC1>



of the m^cC^{223} ammonium nitrogen in the x-ray structure. The ammonium nitrogen of m^cC^{223} in the model (gray ball) deviates by 0.66 Å from the position in the x-ray structure (blue ball). The side chain of Y^{128} , which is shown by gray carbons in the model and blue carbons in the x-ray structure, stabilizes the ammonium group of MTSET via cation–π interactions.

Figure S1. Validating the methodology of predicting the energetically optimal orientation of m^cC^{223} residues with the x-ray structure of Sortase B (PDB code 1QXA). (A) The superposition of the 1,000 minimum energy conformations of m^cC^{223} (gray carbons, yellow sulfur atoms, and blue nitrogen) predicted with the same methodology, which was used to predict orientations of m^cC residues in Ca_{2.1} mutants (see Materials and methods). The protein backbone is shown as smooth ribbons, and the side chain of Y^{128} is shown as sticks. (B) The energetically most favorable orientation of m^cC^{223} side chain (gray) versus the position

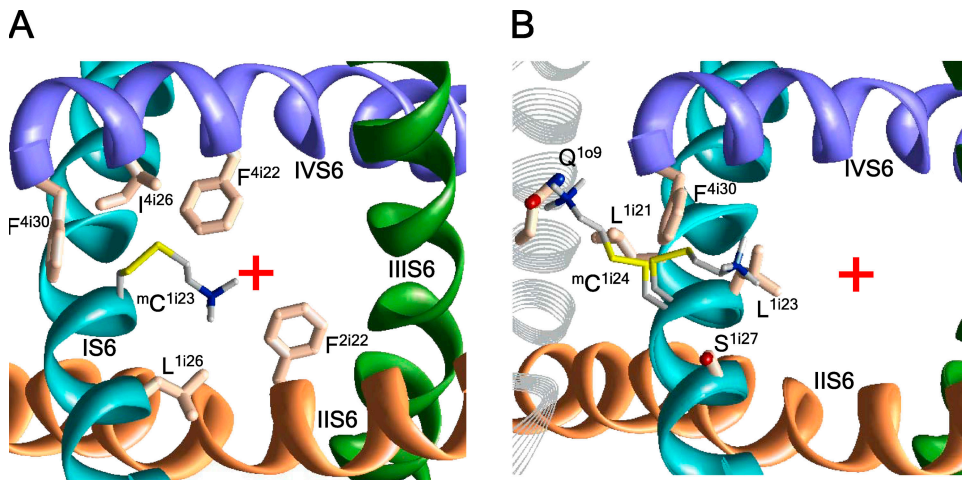


Figure S2. The cytoplasmic views of Ca_v2.1 with MTS-modified cysteines at positions 1i23 and 1i24. The red cross indicates the pore axis. (A) The side chains of L¹ⁱ²⁶, F²ⁱ²², F⁴ⁱ³⁰, F⁴ⁱ²², and I⁴ⁱ²⁶ stabilize ^mC¹ⁱ²³ inside the pore. (B) The side chain of ^mC¹ⁱ²⁴ can adopt two orientations: S¹ⁱ²⁷ and L¹ⁱ²³ stabilize orientation toward the pore, whereas L¹ⁱ²¹, Q^{1o9}, and F⁴ⁱ³⁰ stabilize the repeat interface orientation.

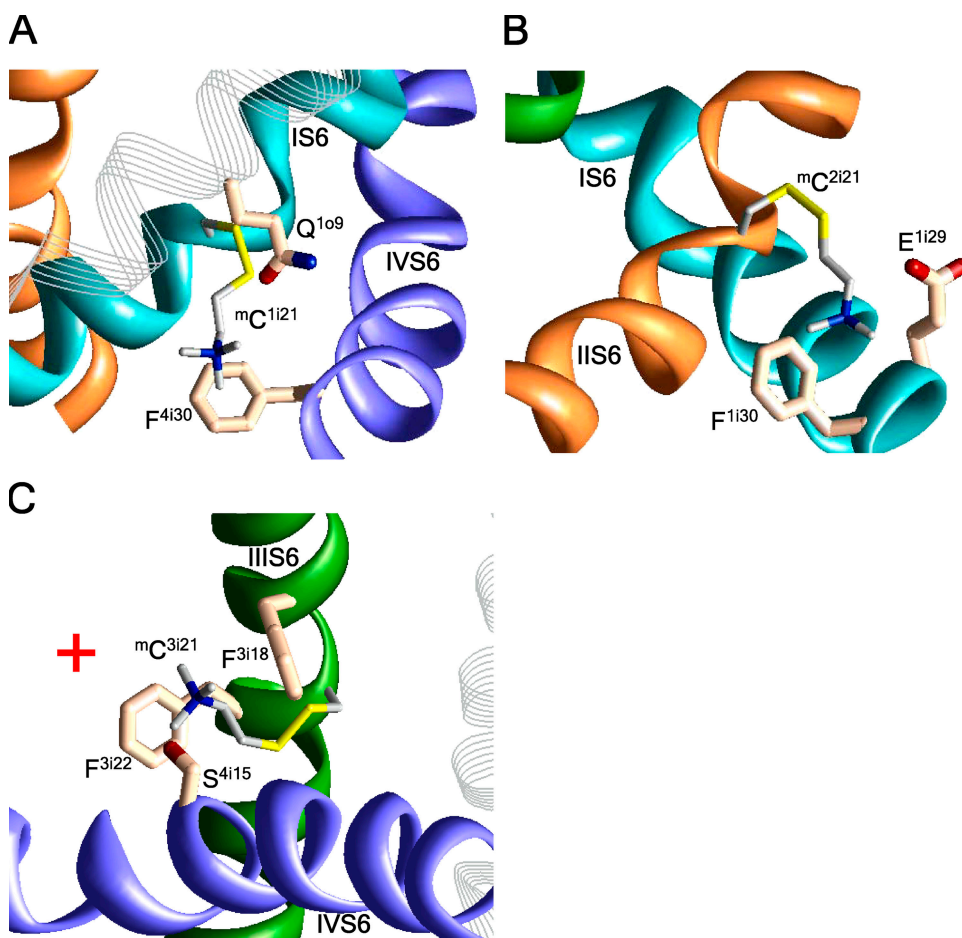


Figure S3. Energetically favorable orientations of ^mC¹ⁱ²¹, ^mC²ⁱ²¹, and ^mC³ⁱ²¹. (A) The side view of ^mC¹ⁱ²¹, which is stabilized in the I/IV repeat interface by cation–π interactions with F⁴ⁱ³⁰. (B) The side view of ^mC²ⁱ²¹, which is stabilized in the I/II repeat interface by cation–π interactions with F¹ⁱ³⁰. (C) The extracellular view of ^mC³ⁱ²¹, which projects to the pore and interacts with F³ⁱ²², F³ⁱ¹⁸, and S⁴ⁱ¹⁵. The red cross indicates the pore axis.

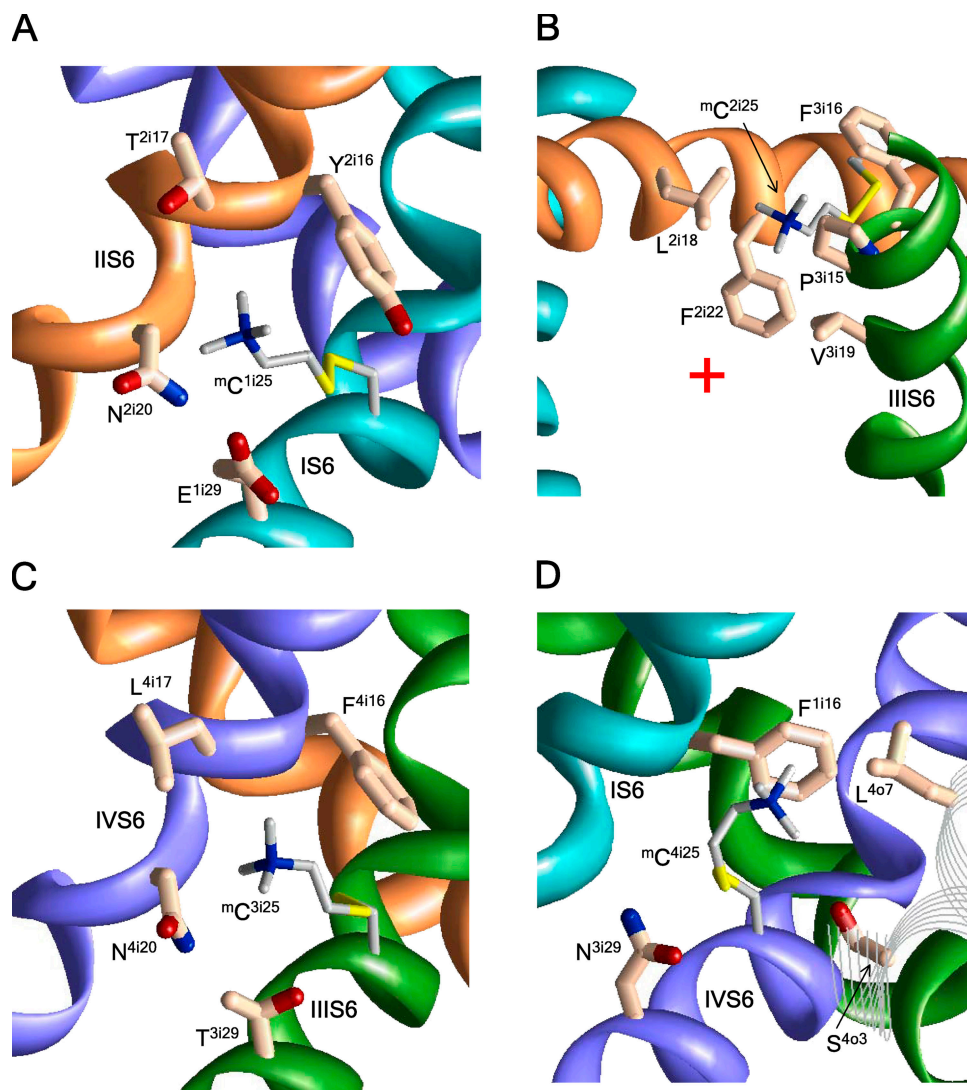


Figure S4. Energetically preferable orientations of residues mC^{i125} . (A, C, and D) Side chains mC^{i125} , mC^{i3125} , and mC^{i4125} face away from the pore, and MTSET does not inhibit the respective channels. The channels are oriented to show residues that interact with the ammonium groups of respective mC residues. (B) The cytoplasmic view of channel mC^{i2125} . The ammonium group of mC^{i2125} approaches the pore, and MTSET inhibits the respective channel. The red cross indicates the pore axis.

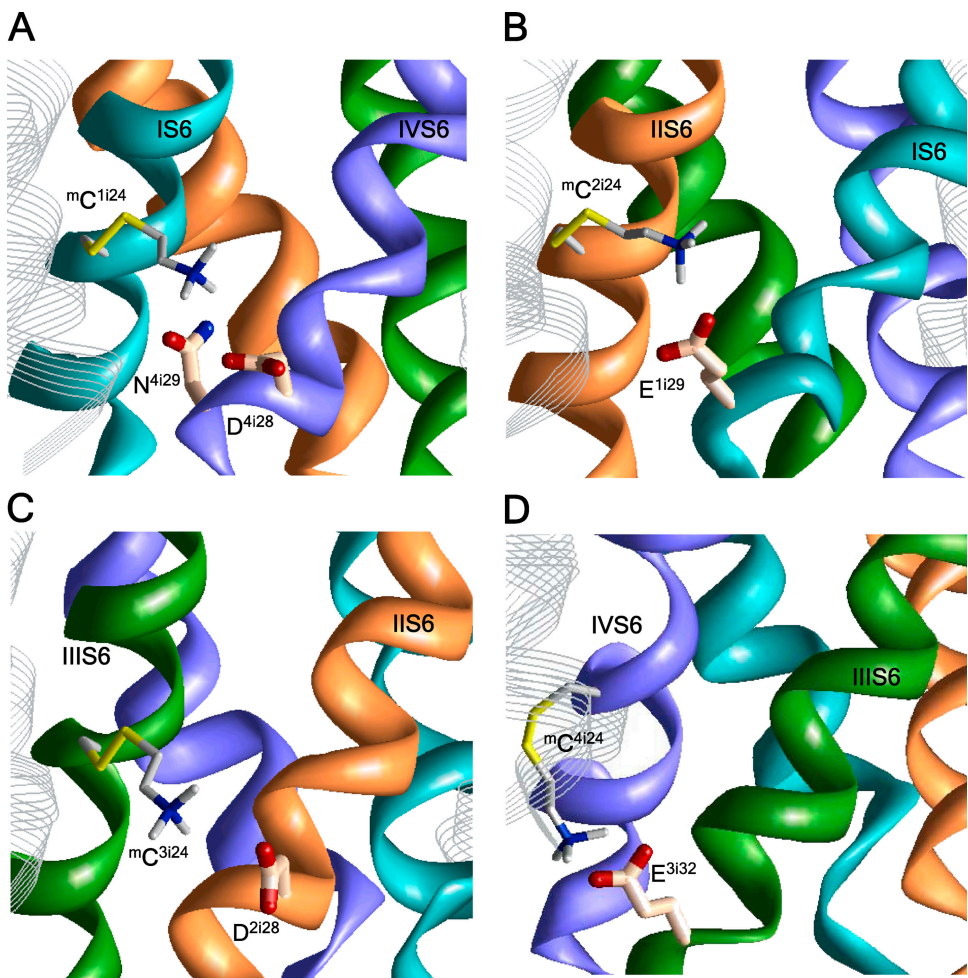


Figure S5. The energetically most favorable orientations of $m^3\text{C}^{124}$ residues in the KcsA-based model of the closed channel $\text{Ca}_2.1$. The ammonium groups of $m^3\text{C}^{124}$ form salt bridges with ionizable residues in the previous subunits. A salt bridge may stabilize the closed conformation of the channel.

Table S1
The current inhibition by MTSET^a and mobility of atoms ^mC-N⁺

Cys in position	Current inhibition	Distance of atom ^m C-N ⁺ from the pore axis		
		%	Å	Å
Control	19.0 ± 5.9			
1i15	45.1 ± 11	1.2	-0.0	+3.3
1i16	37.5 ± 9.5	11.5	-2.3	+0.9
1i17	25.6 ± 10.5	19.4	-5.4	+0.2
1i18	15.3 ± 6.4	11.2	-1.4	+0.3
1i19	57.2 ± 8.3	1.3	-1.3	+1.7
1i21	28.2 ± 8.1	11.7	-0.1	+0.2
1i23	81.2 ± 4.0	1.61	-0.4	+1.3
1i24	86.8 ± 3.7	6.5	-0.0	+1.3
1i25	15.3 ± 3.7	14.8	-0.8	+3.0
2o10	50.0 ^c	8.5	-0.4	+0.9
2i15	43.0 ± 5.5	2.7	-1.8	+1.6
2i16	41.9 ± 12.4	13.8	-0.8	+3.8
2i17	28.4 ± 9.2	17.9	-4.3	+0.6
2i18	85.8 ± 2.6	2.7	-1.7	+1.2
2i19	55.5 ± 8.3	0.5	-0.4	+0.7
2i20	56.2 ± 2.4	3.5 ^d	-0.2	+0.0
2i21	16.6 ± 2.8	13.4	-0.6	+2.9
2i23	87.7 ± 2.3	2.9	-2.1	+1.7
2i24	99.2 ± 1.2	6.9	-0.5	+0.9
2i25	35.6 ± 3.9	7.5	-0.3	+2.0
3o10	15.0 ^c	13.0	-1.1	+0.1
3i15	39.0 ± 9.7	3.8	-1.6	+0.2
3i16	33.2 ± 11.9	15.3	-0.8	+1.6
3i17	27.0 ± 11.9	15.3	-1.6	+1.4
3i18	17.7 ± 6.5	10.3	-1.2	+0.3
3i19	93.0 ± 1.6	0.3	-0.2	+2.1
3i20	42.0 ± 6.4	9.8 ^d	-2.8	+0.0
3i21	39.8 ± 6.1	5.3	-0.0	+0.1
3i23	43.6 ± 9.2	1.9	-0.0	+0.1
3i24	73.6 ± 10.0	7.9 ^d	-1.1	+0.0
3i25	24.0 ± 3.6	14.6	-1.0	+0.3
4o10	95.0 ^c	9.0	-0.8	+1.4
4i15	65.5 ± 9.0	2.5	-0.7	+1.1
4i16	44.1 ± 8.5	10.0 ^d	-0.0	+3.8
4i17	20.5 ± 1.8	14.6	-0.3	+1.7
4i18	31.4 ± 8.8	8.3	-0.0	+1.9
4i19	56.5 ± 12.7	0.3	-0.3	+0.7
4i23	59.4 ± 5.4	1.7	-1.2	+1.4
4i24	100.0 ± 0.0	6.8	-0.0	+1.1
4i25	25.0 ± 6.6	15.0	-0.8	+1.1

^aZhen et al. (2005. *J. Gen. Physiol.* doi:10.1085/jgp.200509292).

^bDeviations from the indicated distance in the apparent global minimum.

^cStandard deviations are not available.

^dFor residues ^mC²ⁱ²⁰, ^mC³ⁱ²⁰, ^mC³ⁱ²⁴, and ^mC⁴ⁱ¹⁶, the distances are shown for the local minima with the energies of 1.5, 1.7, 1.3, and 0.4 kcal/mol from the respective apparent global minima.